

ELIMINATION OF PARITY DOUBLETS

IN REGGE AMPLITUDES

Thesis by

Mark Brecher Kislinger

In Partial Fulfillment of the Requirements

For the Degree of

Doctor of Philosophy

California Institute of Technology

Pasadena, California

1970

(Submitted May 27, 1970)

ACKNOWLEDGEMENTS

During the course of several years as my research advisor, Dr. Richard P. Feynman has taught me how to think, encouraged me, inspired me, and guided me to many fruitful areas of investigation. I am deeply grateful to have such a superb teacher.

I would like to thank Dr. Steven C. Frautschi for his advice and encouragement during the preparation of the papers: "Fermion Reggeization Without Parity Doubling", and "A Regge Amplitude Arising from $SU(6)_W$ Vertices", which were co-authored with R. Carlitz, and which comprise the text of this thesis.

I would also like to thank the National Science Foundation and the California Institute of Technology for financial support.

ABSTRACT

In Part I, the common belief that fermions lying on linear trajectories must have opposite-parity partners is shown to be false. Reggeization of a sequence of positive-parity fermion resonance is carried out in the Van Hove model. As a consequence of the absence of negative-parity states, the partial-wave amplitudes must have a fixed cut in the J plane. This fixed cut, in conjunction with the moving Regge pole, provides a new parametrization for fermion-exchange reactions, which is in qualitative agreement with the data.

In Part II, the spin structure of three particle vertices is determined from the quark model. Using these $SU(6)_W$ vertices in the Van Hove model, we derive a Reggeized scattering amplitude. In addition to Regge poles there are necessarily fixed Regge cuts in both fermion and boson exchange amplitudes. These fixed cuts are similar to those found in Part I, and may be viewed as a consequence of the absence of parity doubled quarks. The magnitudes of the pole and cut terms in an entire class of $SU(6)$ related reactions are determined by their magnitudes in a single reaction. As an example we explain the observed presence or absence of wrong-signature nonsense dips in a class of reactions involving vector meson exchange.

TABLE OF CONTENTS

	<u>Page</u>
Acknowledgements	ii
Abstract	iii
Introduction	v
Part I : Fermion Reggeization Without Parity Doubling	1
Part II : Regge Amplitude Arising from $SU(6)_W$ Vertices	
1. Introduction	7
2. Quark Model and $SU(6)_W$	9
3. Construction of a Regge Amplitude	14
4. Experimental Consequences	18
5. Discussion	22
Part III: Covariant Construction of Quark Graph Amplitudes	23
Tables	38
References	45
Figures	50

INTRODUCTION

The Regge trajectory language has proved to be one in which much of high energy phenomenology can be simply expressed. The simple linear form and almost universal slope, which almost all trajectories seem to have, account for much of the structure of the hadron spectrum and the high energy behavior of many scattering amplitudes. The simplicity of the Regge parameters, which Regge theory alone cannot account for, is certainly a clue to the theoretical substructure of hadrons.

One of the few exact consequences of Regge theory is that fermions lying on a linear trajectory must be accompanied by opposite parity partners. Hence it has always seemed puzzling that there are no opposite parity partners to the known baryons. The only candidates for a parity doublet are the $5/2^+$ and $5/2^-$ baryon octets, but these differ in their F/D ratios. In this thesis we show that a straightforward approach to the problem of fermion reggeization does not lead to the existence of parity doublets. We find that the natural form of a Regge amplitude associated with a sequence of fermion resonances of definite parity is one in which fermion trajectories are in general accompanied by fixed cuts. As an alternative to fixed cuts, one may make the ad hoc assumption that parity doublets exist. The absence of such states is the strongest support for our work. We find that the existence of our

cuts is in qualitative agreement with the data.

We also examine the problem of boson reggeization when the bosons are viewed as quark-antiquark composites. Previous treatments of this problem required that the spin $1/2$ quarks be parity doubled, much as the fermions in fermion reggeization. Again we show that parity doubling the quarks, which would quadruple the number of bosons, is not required in a straightforward approach. We again find that trajectories are accompanied by fixed cuts, this time as a consequence of the absence of parity doubled quarks. The data for a whole class of boson exchange reactions are shown to be in qualitative agreement with the existence of our cuts.

Our approach to reggeization follows that of Feynman and Van Hove, in which a Regge amplitude is expressed as the sum of its pole singularities. Such an amplitude has required analyticity properties, and only the input particles. In other words, we construct a Regge amplitude with the minimum requirements as input. We then abstract from the model the basic characteristics of the amplitude. The major part of this thesis is just applying this approach to the two problems discussed above. Section I is concerned with the problem of fermion reggeization. In Section II we review the quark model and give a simple approach to boson reggeization within the quark model. In Section III we give a more elegant approach to the material of Section 2 and show clearly the connection between fermion reggeization and reggeization of particles which are composites of fermions, i.e., bosons viewed as quark-anti-

quark composites. Section III also gives a simple formulation of our results in terms of quark graphs.

PART I

FERMION REGGEIZATION WITHOUT PARITY DOUBLING

Gribov¹ showed that every fermion Regge trajectory $\alpha^+(W)$ must be accompanied by a MacDowell symmetric² trajectory $\alpha^-(W) = \alpha^+(-W)$ of the opposite parity. If (as is indicated by experiment for N_α and Δ_δ) a trajectory is linear in $u = W^2$, its MacDowell twin will be degenerate with it. Hence it has always seemed puzzling that no parity partners of the N and $\Delta(1238)$ have been found. Attempts to find an analytic form in which states on the MacDowell twin are systematically suppressed have not been successful.³ We deduce the appropriate analytic form from a model containing only resonances of positive parity lying on a linear trajectory. The partial-wave amplitudes are found to have a fixed Regge cut, and the negative-parity (MacDowell twin) trajectory lies on an unphysical sheet of the J plane at positive energies. The idea of a fixed Regge cut is not new; it is present in the solution of the Dirac equation with a Coulomb potential.⁴ In the present problem it is, of course, possible to have parity doubling and no Regge cut; but lacking any a priori reason for parity doubling, we anticipate in general the presence of a fixed Regge cut in fermion-exchange amplitudes.

We will illustrate the origin of the fixed cut in the Van Hove model.⁵ The amplitude in this model is the sum of Feynman diagrams for the exchange of all resonances along a given trajectory. Clearly,

this amplitude satisfies the usual analyticity requirements and contains only the resonances of the input trajectory. In πN scattering, the Feynman diagram for the exchange of a natural-parity ($J^P = 1/2^+, 3/2^-, 5/2^+, \dots$) fermion resonance of spin $J = \ell + 1/2$ and mass $m(\ell)$ in the u channel^{6,7} is

$$\begin{aligned} \bar{u}_2 \mathcal{M}(J) u_1 &= \bar{u}_2 \gamma_5 g^2(\ell) p'_{\mu_1} \dots p'_{\mu_\ell} T_{\mu_1 \dots \mu_\ell; \nu_1 \dots \nu_\ell}^J p_{\nu_1} \dots p_{\nu_\ell} \gamma_5 u_1 \\ &= \bar{u}_2 \frac{g^2(\ell) p^{2\ell} P'_{\ell+1}(z_u)}{u - m^2(\ell)} \left[\frac{k}{m(\ell)} - 1 \right] u_1 + O(z_u^{\ell-1}), \quad (1) \end{aligned}$$

where $T_{\mu, \nu}^J$ is the propagator for a spin- J fermion. We Reggeize by summing a sequence of resonances and transforming the sum into an integral a la Sommerfeld and Watson⁸:

$$\mathcal{M} = \sum_J \mathcal{M}(J) \approx \frac{i}{2} \int d\ell \frac{g^2(\ell) p^{2\ell} P'_{\ell+1}(-z_u)}{(u - m^2(\ell)) \sin \pi \ell} \left[\frac{k}{m(\ell)} - 1 \right]. \quad (2)$$

All terms but those contributing to the leading power of the asymptotic expansion of $\mathcal{M}(u, z_u)$ as $z_u \rightarrow \infty$ have been dropped.

If we take $m^2(\ell) = (\ell - \alpha_0)/\alpha'$ and assume for convenience that $g^2(\ell)$ is analytic in ℓ ,⁹ we can open the contour in the ℓ plane and obtain a contribution from the pole at $m^2(\ell) = u$ and the cut with branch point at $\ell = \alpha_0$ (see Fig. 1). This gives

$$\begin{aligned} \mathcal{M}(u, z_u) &= \frac{\pi g^2(\alpha(u)) p^{2\alpha(u)} P'_{\alpha(u)+1}(-z_u)^{\alpha'}}{\sin \pi \alpha(u)} \left[\frac{k-W}{W} \right] \\ &\quad - k \int_{-\infty}^{\alpha_0} d\ell \frac{g^2(\ell) p^{2\ell} P'_{\ell+1}(-z_u)}{\sqrt{-m^2(\ell)} (u - m^2(\ell)) \sin \pi \ell}, \quad (3) \end{aligned}$$

where $\alpha(u) = \alpha_0 + \alpha' u$. (4)

In the limit $z_u \rightarrow \infty$,

$$\mathcal{M}(u, z_u) \rightarrow \frac{\pi g^2(\alpha(u)) c(\alpha(u)) s^{\alpha(u)} \alpha'}{\sin \pi \alpha(u)} \left[\frac{k-W}{W} \right]$$

$$-k \int_{-\infty}^{\alpha_0} d\ell \frac{g^2(\ell) c(\ell) s^\ell}{\sqrt{-m^2(\ell)} (u - m^2(\ell)) \sin \pi \ell} \quad (5)$$

where $c(\ell) = \frac{\Gamma(2\ell+2)}{4^\ell (\Gamma(\ell+1))^2}$. (6)

The first term of (5) has the form of a Regge pole contribution while the second term has the form of a Regge cut. The singularity at $u=0$ in the residue of the pole term is cancelled by the cut term, so that \mathcal{M} is analytic in u (see Eq. (11)).

The principal features of our solution can be seen in the partial-wave amplitudes $f_{J\pm 1/2}^{\mp}$ (W),² which can be read off directly from (1). We find that

$$f_{J\pm 1/2}^{\mp} = -\frac{E\bar{M}}{8\pi W} \left(\frac{\sqrt{\alpha' u \pm \sqrt{\ell - \alpha_0}}}{\ell - \alpha_0 - \alpha' u} \right) \frac{\alpha'}{\sqrt{\ell - \alpha_0}} p^{2\ell} g^2(\ell) \quad , \quad (7)$$

where $\ell = J - 1/2$. There is a moving pole at $\ell = \alpha(u)$ and a fixed cut at $\ell = \alpha_0$. Note that the moving pole in $f_{J-1/2}^+$ is on the physical sheet of the ℓ plane only for $W < 0$. As we move from $W < 0$ to $W > 0$, the pole at $\ell = \alpha(W^2)$ moves through the fixed cut onto the second sheet of the ℓ plane as shown in Fig. 2; this explains why

there are no negative-parity resonances in our model.

The cut $(\ell - \alpha_0)^{-1/2}$ in (7) is due to the presence of odd powers of $m(\ell)$ in (1). We can obtain a solution with no Regge cut only if we include negative-parity states along with the positive-parity ones. This would correspond to the usual solution; but it clearly involves the ad hoc assumption that the negative-parity states exist.

Unless $g^2(\alpha_0) = 0$, the partial-wave amplitudes (7) have infinities for $\ell \rightarrow \alpha_0$, in violation of unitarity. Of course, our model has zero-width resonances, so it is clearly not unitary. We wish to demonstrate that there exists a smooth limit from the unitarized theory to the zero-width limit, and that this limit should be useful in parametrizing experimental data. The procedure for unitarizing the model has been discussed by Sugar and Sullivan,¹¹ who find that certain fixed poles are converted into moving poles in the process.

In our case¹² the unitarized partial-wave amplitudes have the form

$$f_{J\pm 1/2}^{\mp} = \frac{E \pm M}{8\pi W} \frac{p^{2\ell} g^2(\ell)}{[m(\ell) - g^2(\ell)a(u)] W - [m^2(\ell) + g^2(\ell)b(u)]}, \quad (8)$$

where $a(u)$ and $b(u)$ are functions with the proper right-hand cuts in u . The amplitudes $f_{J\pm 1/2}^{\mp}$ have a fixed cut at $\ell = \alpha_0$ and only moving poles. In particular if $g^2(\ell) = c$, a constant, $f_{J\pm 1/2}^{\mp}$ have two moving poles,¹³ with trajectories $\alpha_{1,2}$ ¹⁴ given by

$$2m(\alpha_{1,2}(u)) = W \pm \sqrt{W^2 - 4cWa(u) - 4cb(u)}. \quad (9)$$

In the limit $a, b \rightarrow 0$, $\alpha_1 \rightarrow \alpha(u)$ (the input positive-parity trajectory) and $\alpha_2 \rightarrow \alpha_0$ (a fixed pole). Thus we can interpret the factor $(\ell - \alpha_0)^{-1/2}$ in (7) as the coincidence of a fixed cut, $(\ell - \alpha_0)^{1/2}$, and a fixed pole, $(\ell - \alpha_0)^{-1}$. When the model is unitarized, the fixed pole becomes a moving pole just as in Ref. 11. Although the pole at $\ell = \alpha_2(u)$ does contribute to the asymptotic scattering amplitude, as long as a and b are small the trajectory $\alpha_2(u)$ will never rise high enough to produce any physical resonances.

Unless $a(u)$ and $b(u)$ are small, the unitarized trajectory will deviate from the linear form (4). Since experiment indicates approximately linear trajectories, we conclude that a and b may be neglected and data may be parametrized using (5).

For small negative u , we make the approximation

$$\frac{g^2(\alpha(u)) c(\alpha(u)) \alpha'}{\sin \pi \alpha(u)} \approx G_0 + G_1 u \quad (10)$$

Then (5) becomes

$$M \approx \pi \left(\frac{G_0}{W} + G_1 W \right) s^{\alpha_0 + \alpha' u} (k - W) - \pi \left[\left(\frac{G_0}{W} + G_1 W \right) s^{\alpha' u} (1 - \text{erf}(\sqrt{\alpha' u \ln s})) - \frac{G_1}{\sqrt{\alpha' \pi \ln s}} \right] s^{\alpha_0} k \quad (11)$$

The first term is clearly a Regge pole, and the second is a fixed Regge cut, since

$$\text{erf}(x) \xrightarrow{|x| \rightarrow \infty} 1 - \frac{1}{\sqrt{\pi}} e^{-x^2} \left[\frac{1}{x} - \frac{1}{2x^3} + \dots \right] \quad |\arg x| < 3\pi/4 \quad (12)$$

We can see explicitly how the singularity in the pole residue is canceled by the cut. The remaining part of the cut term has no \sqrt{u} singularity because erfx is odd in x . Signature may be incorporated in our formulas by the modification

$$\mathcal{M}(u, z_u) \rightarrow \frac{1}{2} [\mathcal{M}(u, z_u) + \tau \mathcal{M}(u, -z_u)].$$

With this modification, the pole term in (11) will acquire the usual signature factor and the cut will have a complicated varying phase.

The strongest experimental support of our work lies in the absence of parity partners to known fermion resonances. Also our conclusion that the partial-wave amplitudes contain a fixed Regge cut does not clash with experiment. Note that by an appropriate choice of G_0 and G_1 , the ratio of the cut contribution to that of the pole can be chosen arbitrarily for a given range of s . If the pole contribution is dominant, we expect to see typical Regge shrinkage and dips where the trajectory passes through wrong-signature nonsense points. When the cut dominates, there will be no shrinkage and no wrong-signature nonsense dips. Nucleon-exchange data support this correlation. In $\pi^+ p$ backward scattering, the data show Regge shrinkage and a marked dip at $u = -0.2$. In backward π^0 photoproduction, there is no shrinkage and no dip at $u = -0.2$.

PART II

REGGE AMPLITUDE ARISING FROM $SU(6)_W$ VERTICES

1. Introduction

The $SU(3)$ symmetry of the quark model has been extremely useful in classifying strongly interacting particles and in predicting the relative strengths of their couplings. Spin has been incorporated in the model to give a successful classification of hadron states under $SU(6)$.¹⁵ The most natural way of treating spin at three particle vertices yields the symmetry $SU(6)_W$.^{16,17} While this symmetry correctly describes many vertices,¹⁷ there has previously been no successful application to scattering¹⁸ amplitudes.

In this thesis we determine the form of the Regge amplitude which results from assuming $SU(6)_W$ as a vertex symmetry. Knowledge of vertices involving a spin J resonance enables us to construct the Feynman amplitude for the exchange of the resonance. Then, using the Van Hove model,⁵ we can express the Regge amplitude as a formal sum (on J) of such resonance exchanges. Hence in this model, the form of the Regge amplitude is determined by the assumption of $SU(6)_W$ symmetric vertices. We find that Regge poles are, in general, accompanied by fixed Regge cuts, with branch points at the zero energy intercept of the trajectory. These fixed cuts are similar to those suggested in Part I of this thesis for fermion exchange amplitudes as a

consequence of the absence of parity doubled fermion states. The fixed cuts found here for meson (quark-antiquark) exchange amplitudes may be viewed as a consequence of the absence of parity doubled quarks.¹⁹

The presence of significant fixed cut terms has important experimental consequences. The shrinkage characteristic of a Regge trajectory with normal slope will be absent in those amplitudes which have fixed cuts, and there will be no dips at wrong-signature nonsense points along the trajectory. Given the magnitudes of pole and cut terms in some reaction, we are able to predict the magnitudes of these terms for a whole class of $SU(6)$ related reactions. Applying our approach to a set of vector meson exchange processes, we find that the numerical importance of cut terms--as indicated by the presence or absence of wrong-signature nonsense dips in differential cross sections--is in accord with our predictions.

An outline of Part II of this thesis is as follows. In Section 2 we show that $SU(6)_W$ is the natural vertex symmetry arising from the quark model and remind the reader how to calculate $SU(6)_W$ vertices. Construction of a Regge amplitude from the $SU(6)_W$ vertices is carried out in Section 3. Some consequences of our approach are given in Section 4, with particular attention to the question of wrong-signature nonsense dips. A discussion of our work is given in Section 5 with some suggestions for further research on this problem.

2. The Quark Model and $SU(6)_W$

The classification of baryons as qqq composites and mesons as $q\bar{q}$ composites implies that any $SU(3)$ invariant vertex may be pictorially represented by quark graphs. (See Fig. 3.) These graphs are drawn according to the following rules: (a) Each quark or antiquark is represented by a directed line. (b) A baryon or antibaryon is represented by three lines running in the same direction. (c) A meson is represented by two lines running in opposite directions. Zweig²⁰ suggested an additional rule: (d) The quark and antiquark lines of a single meson should not be connected. (This rule accounts for the absence of the decay $\phi \rightarrow \rho\pi$ and the weak coupling of the ϕ to nucleons.) Note that the rules (a) - (d) are precisely those used by Harari²¹ and Rosner²² to construct their duality diagrams.

We wish to incorporate spin into the quark graph picture in the simplest possible fashion. We choose a Lorentz frame in which the particle momenta are collinear along the z axis. In such a frame, we assume that the spins of quarks a , b , and d (in Fig. 3) are unchanged in the reaction. How, then, must the spins of the annihilating quarks c and e be related? The parity of a $q\bar{q}$ pair is $-(-1)^L$, so if parity is to be conserved, q_c and \bar{q}_e must annihilate in an odd angular momentum state. Then angular momentum conservation requires that $L = 1$ and that the quark spins form a triplet. If, furthermore, the transverse motions of the annihilating quarks may be neglected, then the quark momenta lie along the z axis, so $L_z = 0$ and hence $S_z = 0$.

Thus we see that the $\bar{q}q$ state annihilates with the quark spins in a triplet state, $S = 1$, $S_z = 0$. This is exactly the result given by the collinear symmetry $SU(2)_W$.¹⁶ Taking into account the $SU(3)$ quantum numbers of the quarks, we obtain $SU(6)_W$ as the natural vertex symmetry of the quark model.²³ Note that the derivation above is independent of what collinear frame we choose, since $SU(2)_W$ states are invariant under boosts along the z axis.

Choosing some collinear frame, it is easy to calculate the $SU(6)_W$ symmetric vertex functions. Let each quark be represented by a pair of indices (α, \underline{a}) , where α specifies its $SU(3)$ nature and \underline{a} gives its spin orientation along the z axis. In a collinear frame, the meson-baryon vertex (Fig. 3) has the form

$$\bar{B}_{(\alpha a)(\beta b)(\gamma c)} B^{(\alpha a)(\beta b)(\delta d)} M^{(\gamma e)}_{(\delta d)} D_{ec} \quad (1)$$

The matrix

$$D = \frac{1}{\sqrt{2}} \begin{pmatrix} 0 & 1 \\ 1 & 0 \end{pmatrix} \quad (2)$$

in (1) specifies that q_c and \bar{q}_e annihilate in a spin state $S = 1$, $S_z = 0$.

Let us recall the form of the $SU(6)$ wave functions²⁴ for the 56 baryons, $B^{(\alpha a)(\beta b)(\gamma c)}$, and the 35 mesons, $M^{(\alpha a)}_{(\beta b)}$.

$$B^{(\alpha a)(\beta b)(\gamma c)m} = \frac{1}{3} \left[\epsilon^{\alpha\beta\sigma} B^\gamma{}_\sigma C_{ab} \chi_c^{(m)} + \epsilon^{\beta\gamma\sigma} B^\alpha{}_\sigma C_{bc} \chi_a^{(m)} + \epsilon^{\gamma\alpha\sigma} B^\beta{}_\sigma C_{ca} \chi_b^{(m)} \right] + D^{\alpha\beta\gamma} (\sigma^i C)_{ab} \xi_{ci}^{(m)} \quad (3)$$

The superscript $m = a+b+c$ gives the spin projection of the baryon. χ is a two-component spinor

$$\chi^{(+1/2)} = \begin{pmatrix} 1 \\ 0 \end{pmatrix} \quad ; \quad \chi^{(-1/2)} = \begin{pmatrix} 0 \\ 1 \end{pmatrix} \quad (4)$$

and $\xi_a^{(m)}$ is a vector-spinor,

$$\xi_a^{(m)} = \sum_{\sigma\rho} \left(\frac{1}{2} \sigma, 1\rho \mid \frac{3}{2} m \right) \chi_a^{(\sigma)} \epsilon^{(\rho)} \quad , \quad (5)$$

where

$$\begin{aligned} \epsilon^{\pm 1} &= \frac{1}{2} (\mp 1, -i, 0) \quad , \\ \epsilon^0 &= (0, 0, 1) \quad . \end{aligned} \quad (6)$$

The matrix C is given by

$$C = i \sigma_y = \begin{pmatrix} 0 & 1 \\ -1 & 0 \end{pmatrix} \quad . \quad (7)$$

$B^\alpha{}_\beta$ and $D^{\alpha\beta\gamma}$ are the SU(3) matrices for the octet and decuplet:

$$B^\alpha{}_\beta = \begin{pmatrix} \frac{1}{\sqrt{2}} \Sigma^0 + \frac{1}{\sqrt{6}} \Lambda^0 & & \Sigma^+ & \rho \\ & \Sigma^- & & n \\ & & -\frac{1}{\sqrt{2}} \Sigma^0 + \frac{1}{\sqrt{6}} \Lambda^0 & \\ & & & \Xi^0 \\ & & & & -\frac{2}{\sqrt{6}} \Lambda^0 \end{pmatrix} \quad , \quad (8)$$

$$\begin{aligned}
D^{111} &= \Delta^{++} & D^{112} &= \frac{1}{\sqrt{3}} \Delta^+ \\
D^{113} &= \frac{1}{\sqrt{3}} \Sigma^{*+} & D^{122} &= \frac{1}{\sqrt{3}} \Delta^0 \\
D^{123} &= \frac{1}{\sqrt{6}} \Sigma^{*0} & D^{133} &= \frac{1}{\sqrt{3}} \Xi^0 \\
D^{222} &= \Delta^- & D^{223} &= \frac{1}{\sqrt{3}} \Sigma^{*-} \\
D^{233} &= \frac{1}{\sqrt{3}} \Xi^- & D^{333} &= \Omega^-
\end{aligned} \tag{9}$$

The meson wave function is

$$M_{(\beta\beta)}^{(\alpha\alpha)m} = P_{\beta}^{\alpha} C_{ab} + V_{\beta}^{\alpha} \epsilon_i^{(m)} (\sigma^i C)_{ab}, \tag{10}$$

where

$$P_{\beta}^{\alpha} = \begin{pmatrix} \frac{1}{\sqrt{2}} \pi^0 + \frac{1}{\sqrt{6}} \eta^0 & \pi^+ & K^+ \\ \pi^- & -\frac{1}{\sqrt{2}} \pi^0 + \frac{1}{\sqrt{6}} \eta^0 & K^0 \\ K^- & \bar{K}^0 & -\frac{2}{\sqrt{6}} \eta^0 \end{pmatrix} \tag{11}$$

and

$$V_{\beta}^{\alpha} = \begin{pmatrix} \frac{1}{\sqrt{2}} (\omega^0 + \rho^0) & \rho^+ & K^{*+} \\ \rho^- & \frac{1}{\sqrt{2}} (\omega^0 - \rho^0) & K^{*0} \\ K^{*-} & \bar{K}^{*0} & \phi \end{pmatrix} \tag{12}$$

The superscript m specifies polarization for the vector meson nonet.

Using (3) and (10) in (1), we obtain the vertex functions given in Table I. The $56-56-35$ vertices are all determined to within a single constant factor by the $SU(6)_W$ symmetry. Similarly, the $35-35-35$ vertices may be computed from the coupling

$$M^{1(\alpha a)}_{(\beta b)} M^{2(\beta b)}_{(\gamma c)} M^{3(\gamma d)}_{(\alpha a)} D_{cd} \quad (13)$$

The results are summarized in Table 2.

Using the information in Tables 1 and 2, it is a straightforward matter to calculate the invariant vertex functions which, in a collinear frame, reduce to those given in the Tables. These invariant vertex functions are listed in Table 3.²⁵ Common mass factors have been absorbed in the constants c and d to give the entries a simple form.

The extension of the couplings in Table 3 to vertices involving Regge recurrences of the listed states is easily made. For example, the $SU(6)_W$ symmetric coupling of two pseudoscalar mesons to a V recurrence (quark spin 1) of spin $J = L + 1$ will be

$$-d(J)M_3^{(J)}\epsilon_{3\nu\mu_1\dots\mu_L}^{(p_1+p_2)}_{\nu}{}^{(p_1+p_2)}_{\mu_1}\dots{}^{(p_1+p_2)}_{\mu_L} \left[\langle P_1 P_2 V \rangle - \langle P_1 V P_2 \rangle \right]$$

(ϵ denotes the polarization of the V recurrence.) The higher spin indices simply couple to appropriate momentum factors. In general, couplings for excited states with a given quark spin assignment may be

constructed by decomposing the spin of the states into quark spin and orbital angular momentum and coupling the quark spin according to $SU(6)_W$. This will give a unique result whenever two of the states have no orbital excitation. In other cases there will be more than a single coupling for each class of $SU(6)$ -related reactions.

Note the presence in Table 3 of factors involving the masses M_1 , M_2 , M_3 . These factors have a simple kinematic origin. Some of these, e.g., $(M_1 + M_2)^2 - M_3^2$, arise because the $SU(6)_W$ symmetry relates vertices involving different angular momenta. Other factors, e.g., M_3 in the $P_1 P_2 V$ vertex, arise because the symmetry relates vertices involving vector mesons of different helicities. The polarization vector for a vector meson of zero helicity is proportional to $1/M_V$.²⁶ Hence, within a class of vertices related by $SU(6)_W$, those vertices involving a zero helicity vector meson will contain an extra factor of M_V relative to those not involving a zero helicity vector meson. This is the only source of odd powers of meson mass; the angular momentum factors will always contain factors of (meson mass)².

3. Construction of a Regge Amplitude

The presence of extra "kinematic" factors in the vertex functions has important consequences when we construct a Regge amplitude. In general, we find the presence of fixed Regge cuts with branch points coinciding with the zero energy intercepts of the Regge trajectories.

This phenomenon has been discussed previously for fermion exchange processes; here we find cuts for boson or fermion exchange processes and predict the relative strengths of the cuts in different processes.

The Van Hove model²⁷ expresses a Regge amplitude as a formal sum of Feynman diagrams for the exchange of all resonances along a given trajectory.²⁸ Consider, for example, the reaction

$$\pi^+ + \pi^- \rightarrow \pi^0 + \omega^0 \quad ,$$

mediated by ρ exchange (see Fig. 4). The coupling at a $\omega\rho^*\pi$ vertex is

$$-i\sqrt{2} d(J) \epsilon^{\alpha\mu_1\gamma\delta} \epsilon_{(\omega)\alpha}^* P_{(\rho^*)\gamma} P_{(\pi)\delta} P_{(\pi)\mu_2} \dots P_{(\pi)\mu_J} 2^J \epsilon_{(\rho^*)\mu_1\mu_2\dots\mu_J} \quad ; \quad (14)$$

for a ρ^* of spin J. The $\pi\rho^*$ coupling is

$$-\sqrt{2} d(J) m_{\rho^*} (J) P_{(\pi)\mu_1} P_{(\pi)\mu_2} \dots P_{(\pi)\mu_J} 2^J \epsilon_{(\rho^*)\mu_1\mu_2\dots\mu_J} \quad . \quad (15)$$

The Feynman diagram for the exchange of a ρ^* of a spin J is therefore

$$\mathcal{M}(J) = 2id^2(J) m(J) 4^J \times \left(\frac{P_{\mu_1}^+ \dots P_{\mu_J}^+ T^{(J)}_{\mu_1 \dots \mu_J; \nu_1 \dots \nu_J} P_{\delta}^- P_{\nu_2}^- \dots P_{\nu_J}^- Q_{\gamma} \epsilon_{(\omega)\alpha}^* \epsilon^{\alpha\nu_1\gamma\delta}}{t - m^2(J)} \right)$$

$$= \frac{2id^2(J)m(J)4J}{t - m^2(J)} \epsilon_{(\omega)\alpha}^* Q_\gamma p_\delta^- \epsilon^{\alpha\beta\gamma\delta} \frac{1}{J} \frac{\partial}{\partial p_\beta^-} \mathcal{P}_J(p^+, p^-) , \quad (16)$$

where $T_{\mu;\nu}^{(s)}/(t - m^2(J))$ is the Feynman propagator for a particle of spin J ,

$$\mathcal{P}_J(p^+, p^-) = 4^J (|p^+||p^-|)^J P_J \left(\frac{p^+ \cdot p^-}{|p^+||p^-|} \right) , \quad (17)$$

and $t = Q^2$. We assume that $m_\pi = m_\omega$ to simplify the kinematics.

Summing over J and transforming the sum into a contour integral gives

$$\mathcal{M} = \sum_J \mathcal{M}(J) = \frac{1}{2} Z_\beta \int_C dJ \frac{d^2(J)m(J)}{t - m^2(J)} \frac{1}{J} \frac{\partial}{\partial p_\beta^-} \frac{\mathcal{P}_J(p^+, -p^-)}{\sin \pi J} , \quad (18)$$

using the abbreviation

$$Z_\beta = 2i \epsilon_{(\omega)\alpha}^* Q_\gamma p_\delta^- \epsilon^{\alpha\beta\gamma\delta} . \quad (19)$$

The contour C is indicated in Fig. 5. If we assume that the m^2 is a linear function of J ,

$$m^2(J) = \frac{J - \alpha_0}{\alpha'} , \quad (20)$$

and that $d^2(J)$ is analytic, then we can open the contour in the J plane obtaining contributions from the pole at $m^2(J) = t$ and the cut with branch point $J = \alpha_0$. This gives

$$\mathcal{M} = \frac{\pi d^2(\alpha) \sqrt{t} \alpha'}{\sin \pi \alpha} z_\beta \frac{1}{J} \frac{\partial}{\partial p_\beta^-} \mathcal{P}_J(p^+, -p^-)$$

$$- z_\beta \int_{-\infty}^{\alpha_0} dJ \frac{d^2(J) \sqrt{-m^2(J)}}{(t - m^2(J)) \sin \pi J} \frac{1}{J} \frac{\partial}{\partial p_\beta^-} \mathcal{P}_J(p^+, -p^-) \quad (21)$$

where $\alpha(t) = \alpha_0 + \alpha' t$. (22)

In the limit $s = (p^+ + p^-)^2 \rightarrow \infty$,

$$\mathcal{M} \rightarrow \frac{\pi d^2(\alpha(t)) b(\alpha(t)) \alpha' s^{\alpha(t)-1}}{\sin \pi \alpha(t)} z_\beta p_\beta^+ \sqrt{t}$$

$$- z_\beta p_\beta^+ \int_{-\infty}^{\alpha_0} dJ \frac{d^2(J) \sqrt{-m^2(J)} b(J) s^{J-1}}{(t - m^2(J)) \sin \pi J} \quad (23)$$

where

$$b(J) = \frac{\Gamma(2J+1)}{(\Gamma(J+1))^2} \quad (24)$$

It is clear that (23) consists of a moving Regge pole term and a fixed Regge cut. Nonsense couplings along the trajectories are presumably eliminated in the usual way by zeros of $d^2(J)$ at $J=0, -1, -2, \dots$. Therefore, for negative t , we can approximate

$$\frac{d^2(\alpha(t)) b(\alpha(t)) \alpha'}{\sin \pi \alpha(t)} = d_0 \quad (25)$$

Then (23) becomes

$$\begin{aligned} \mathcal{M} &\approx \pi d_o z_\beta p_\beta^+ \left[\sqrt{t} \operatorname{erf}(\sqrt{\alpha' t \ln s}) s^{\alpha(t)-1} + \frac{1}{\sqrt{\alpha' \pi \ln s}} S^{\alpha_o-1} \right] \\ &\approx \pi d_o z_\beta p_\beta^+ \left[\sqrt{t} s^{\alpha(t)-1} + \frac{S^{\alpha_o-1}}{2t \sqrt{\pi} (\alpha' \ln s)^{3/2}} \left(1 + \sigma\left(\frac{1}{\alpha' t \ln s}\right) \right) \right]. \end{aligned} \quad (26)$$

In Eq. (18) it is clear that the fixed cut arises from the presence of an odd power of $m(J)$ and the assumption that $d^2(J)$ is even in $m(J)$, i.e., analytic in J . If, for example, $d^2(J) = m(J) d_1(J)$, with $d_1(J)$ analytic, then the $\pi\pi \rightarrow \pi\omega$ amplitude would have no fixed cuts. In this case, however, there would be fixed cuts in the amplitudes $\pi\pi \rightarrow \pi\pi$ and $\pi\omega \rightarrow \pi\omega$. Hence the presence of fixed cuts in some amplitudes is inescapable.

4. Experimental Consequences

The presence of fixed Regge cuts has three important experimental consequences. (1) Asymptotic behavior. At sufficiently high energies, the Regge cut term gives an energy falloff independent of t .²⁹ (2) Polarization. When signature is incorporated in the model by the replacement

$$\mathcal{M}(t, z_t) \rightarrow \frac{1}{2} \left[\mathcal{M}(t, z_t) + \tau \mathcal{M}(t, -z_t) \right], \quad (27)$$

Regge pole terms will acquire the usual Regge phase, but cut terms will have some complicated varying phase. Thus there can be interference between the pole and cut terms, and exchange of a single Regge trajectory will be able to give non-zero polarization. (3) Wrong-signature nonsense dips. The contribution from a single Regge pole term vanishes when the trajectory passes through a nonsense value of the wrong-signature. The cut term does not vanish, however, so an amplitude with a significant cut term will show no dip at wrong-signature nonsense points.³⁰

A qualitative discussion of the third point is easy to make. We will restrict our attention to processes involving vector meson exchange. In Section I we gave a simple criterion for determining the presence of odd powers of M_V in vector meson vertices. The argument required examining the vertex in a collinear frame. Note that the t-channel center-of-mass frame is collinear for both vertices, so we can apply the argument of Section 2 directly to t-channel helicity amplitudes. The factors of $m(J)$ which will appear in t-channel helicity amplitudes involving various ρ^* or ω^* vertices are given in Table 4. Assuming the absence of a cut term in some particular helicity amplitude, this Table allows us to predict the presence or absence of cut terms in other helicity amplitudes. In general, a reaction will have no cuts in some amplitudes and cuts in others. We must pay attention to the relative

magnitudes of the different amplitudes in order to assess the importance of cut terms in any given process.

In Table 5 we tabulate the magnitudes of the helicity amplitudes and the factors of $m(J)$ which lead to Regge cuts for a number of reactions³¹ involving the vertices of Table 4. The relative magnitudes of the contribution of a spin J V^* exchange to the various t -channel helicity amplitudes are given by

$$f_{\lambda\mu}(t=m^2(J),s) = V_1^{(\lambda)} V_2^{(\mu)} \epsilon_1^{(\lambda)*} \cdot \epsilon_2^{(\mu)} G(J) . \quad (32)$$

$V_1^{(\lambda)}$ and $V_2^{(\mu)}$ are the $SU(6)_W$ vertex coefficients from Tables 1 and 2, and $\epsilon_2^{(\mu)}$ specify the orientation of the quark spin of the V^* at vertices 1 and 2 respectively in the t -channel center-of-mass. Equation (32) is obvious for $J = 1$ and is valid for arbitrary J because the higher spin indices always couple to additional momentum factors at each vertex. In the limit $s \rightarrow \infty$,

$$|\epsilon_1^{(\lambda)} \cdot \epsilon_2^{(\mu)}| \rightarrow |\epsilon_1^{(0)*} \cdot \epsilon_2^{(0)}| / (\sqrt{2})^{|\lambda| + |\mu|} .$$

In Table 5, then, we tabulate simply

$$|V_1^{(\lambda)} V_2^{(\mu)} c(J) d(J) / (\sqrt{2})^{|\lambda| + |\mu|}| .$$

For convenience, we have defined

$$g(J) = \frac{c(J) d(J)}{36 m(J)} .$$

Genuine kinematic factors (kinematics of $\pi N \rightarrow \pi N$ are assumed for all reactions listed) are tabulated as \sqrt{t} or t . The factors of $m(J)$ induced by $SU(6)_W$ are determined from Table 4 and tabulated in the appropriate helicity amplitudes.

The qualitative features of the data for the reaction $\pi^- p \rightarrow \pi^0 n$ indicate that the reaction is dominated by a Regge pole in the t -channel helicity 1 amplitude. Therefore, the function $g(J)$ in Table 5 must be approximately even in $m(J)$, i.e., analytic in J , so that the helicity 1 amplitude is purely a Regge pole term while the helicity 0 amplitude contains a Regge cut as well. This cut arises from the presence in the amplitude of a factor $m(J)$ and is referred to in Table 5 as a weak cut. As can be seen in (26), the contribution to the scattering amplitude of a weak cut ($m(J) g(J)$) at $t = 0$ is suppressed by a factor $(\pi \alpha' \ln s)^{-1/2}$ relative to a pole term ($g(J)$). A cut arising from the presence of a factor $1/m(J)$ is referred to as a strong cut. The magnitude of a strong cut ($g(J)/m(J)$) is larger than that of a weak cut by a factor of $2 \alpha' \ln s$.

Now in Table 5 we see that the helicity 1 amplitude in $\pi^- p \rightarrow \omega n$ contains a strong cut with a numerical coefficient larger than that for the pole term in the helicity 0 amplitude. Therefore, in this reaction, the cut effects should be appreciable and we expect no wrong-signature nonsense dip. Proceeding in this manner,

we may make the other predictions given in the last column of Table 5. These predictions agree with experiment for all the reactions listed.³²

5. Discussion

The qualitative discussion above should be largely unaffected by the manner in which the $SU(6)$ symmetry of our theory is broken. Symmetry breaking will alter the $SU(3)$ factors and numerical coefficients in Table 3, but will not affect the mass factors, which arise solely from kinematic considerations. In Table 5 it is apparent that the question of dip or no dip depends primarily on these mass factors. In a quantitative fit of differential cross sections and polarization phenomena, symmetry breaking effects will be important and a more detailed theory will be necessary.

Aside from symmetry breaking, an important question concerns the relation of our work to duality. Since both schemes are based on identical quark graphs, it seems likely that they may be fused in a unified approach.

PART III

COVARIANT CONSTRUCTION OF QUARK GRAPH AMPLITUDES

In Part II we described mesons as quark-antiquark composites and baryons as three quark composites by using non-relativistic $SU(6)$ wave functions for quarks, and writing the hadron wave function as an outer product of the $SU(6)$ wave function of the constituent quarks. Vertex amplitudes for a collinear frame were then calculated with these wave functions, and the corresponding relativistic form of each amplitude was guessed. "Guessing" involved writing all possible invariant vertex couplings, evaluating them in a collinear frame, and solving algebraically for the combination which produced the collinear amplitude. A much simpler approach is to start with covariant wave functions and use them to directly calculate the invariant vertex amplitudes. In this section we shall construct such covariant wave functions. We shall also demonstrate that our results of Section II on the existence of cuts in meson exchange amplitudes can be understood simply from the form of the covariant wave functions.

Since the quarks are fermions, the covariant wave function for a hadron will be an outer product of Dirac spinors, one for each quark or antiquark composing the hadron. The Dirac spinors involve momentum and we must therefore decide what momentum is to appear in each Dirac spinor. Recall that the essential assumption made in the non-relativistic calculation was that the transverse momenta of the quarks could be neglected. Our covariant wave functions must therefore be an

invariant formulation of this assumption, which we make as follows:

"The momentum in the Dirac spinor for each quark is parallel to the momentum of the composite hadron." The magnitude of this momentum is fixed, provided we normalize our Dirac spinors to $\bar{u} u = 1$. That's all there is to it. To construct hadron wave functions, we just sum over the different quark spin projections needed to form a state of definite total spin. It turns out that the resulting expressions can be written quite simply, much as the expression $\sum_{\sigma} u_{\sigma} \bar{u}_{\sigma}$ may be written simply $\frac{\not{P} + M}{2M}$. In what follows we shall be mainly interested in constructing the spin part of the hadron wave function and in so doing we shall neglect the SU(3) quantum numbers of the quarks. We will then form complete wave functions from the outer product of the spin and SU(3) wave functions.

The first thing we shall do is list the Dirac spinors used in describing quarks or antiquarks belonging to a hadron of momentum P and mass M . They are

$$u_{+} = \frac{(\not{P} + M)}{\sqrt{2M(E + M)}} \begin{pmatrix} 1 \\ 0 \\ 0 \\ 0 \end{pmatrix} \quad u_{-} = \frac{(\not{P} + M)}{\sqrt{2M(E + M)}} \begin{pmatrix} 0 \\ 1 \\ 0 \\ 0 \end{pmatrix}$$

$$v_{+} = \frac{(\not{P} - M)}{\sqrt{2M(E + M)}} \begin{pmatrix} 0 \\ 0 \\ 0 \\ 1 \end{pmatrix} \quad v_{-} = \frac{(\not{P} - M)}{\sqrt{2M(E + M)}} \begin{pmatrix} 0 \\ 0 \\ -1 \\ 0 \end{pmatrix}$$

We shall now construct the meson wave functions, which are of the form $u(P)_{\sigma_1} \bar{v}(P)_{\sigma_2}$, where we sum over the values of σ_1 and σ_2 needed to give the desired spin of the meson. For example,

$\frac{u(P)_+ \bar{v}(P)_- - u(P)_- \bar{v}(P)_+}{\sqrt{2}}$ represents a quark-antiquark in a spin-

zero state, and is therefore the wave function for a pseudoscalar meson. We simplify this expression as follows:

$$\begin{aligned} & \frac{u(P)_+ \bar{v}(P)_- - u(P)_- \bar{v}(P)_+}{\sqrt{2}} = \\ & = \frac{(\not{P} + M)}{\sqrt{2} 2M (E + M)} \left\{ \begin{pmatrix} 1 \\ 0 \\ 0 \\ 0 \end{pmatrix} (0 \ 0 \ 1 \ 0) - \begin{pmatrix} 0 \\ 1 \\ 0 \\ 0 \end{pmatrix} (0 \ 0 \ 0 \ -1) \right\} (\not{P} - M) \\ & = \frac{(\not{P} + M)}{2 \sqrt{2} M (E + M)} \begin{pmatrix} 0 & 0 & 1 & 0 \\ 0 & 0 & 0 & 1 \\ 0 & 0 & 0 & 0 \\ 0 & 0 & 0 & 0 \end{pmatrix} (\not{P} - M) \\ & = \frac{1}{\sqrt{2}} \frac{(\not{P} + M)(1 + \gamma_0) \gamma_5 (\not{P} - M)}{4M (E + M)} \\ & = - \frac{((\not{P} + M) \gamma_5)_{m_1 m_2}}{2\sqrt{2} M} \end{aligned}$$

This is the covariant spin part of the pseudoscalar meson wave function. The value of a matrix element for a specific value of the indices m_1, m_2 , is simply the amplitude for the Dirac spinors of the quark and antiquark to have their indices equal to m_1 and m_2 respectively.

In a similar fashion, and with only slightly more work, we will now construct the spin part of the vector meson wave function.

The wave functions for the three vector meson spin states are

$$\frac{1}{\sqrt{2}} (u(P)_+ \bar{v}(P)_- + u(P)_- \bar{v}(P)_+) \quad S_2 = 0$$

$$\bar{u}(P)_+ \bar{v}(P)_+ \quad S_2 = 1$$

$$\bar{u}(P)_- \bar{v}(P)_- \quad S_2 = -1$$

If we're clever, we may write these in the form

$$\epsilon_\lambda^i (M) \frac{(\sigma^i C)_{\sigma_1 \sigma_2}}{\sqrt{2}} u_{\sigma_1} \bar{v}_{\sigma_2} .$$

Here we have used σ^i , the 2 x 2 Pauli matrices, the matrix $C = \begin{pmatrix} 0 & 1 \\ -1 & 0 \end{pmatrix}$, and $\epsilon_\lambda (M)$, the spin polarization vectors for a meson at rest. The values of $\epsilon_\lambda (M)$ are $\epsilon_0 (M) = (0001)$, $\epsilon_{+1} (M) = \frac{1}{\sqrt{2}} (0 -1 -i 0)$, $\epsilon_{-1} = \frac{1}{\sqrt{2}} (0 1 -i 0)$. In trying such a form, we are guessing that a simple form for the vector meson wave function can be written using the polarization vectors. This means that we really want the polarization vectors for a meson of momentum P, rather than one at rest. Before we change, we write our expression in terms of γ matrices, as before.

$$\epsilon_\lambda^i (M) \frac{(\sigma^i C)_{\sigma_1 \sigma_2}}{\sqrt{2}} u_{\sigma_1} \bar{v}_{\sigma_2} = - \epsilon_\lambda^u (M) \frac{(\not{P} + M) \gamma_\mu (1 - \gamma_0) (\not{P} - M)}{4M (E + M) \sqrt{2}}$$

$$= - \epsilon_{\lambda}^{\mu} (M) \frac{(M + \not{P} \gamma_0) \gamma_{\mu} (M + \gamma_0 \not{P}) \left(\frac{\not{P}}{M} - 1\right)}{4M (E + M) \sqrt{2}}$$

Now we switch to the physical spin polarization vectors, $\epsilon_{\lambda}^{\nu} (P)$, using the relation $\Lambda_{\mu}^{\nu} \epsilon_{\lambda}^{\mu} (M) = \epsilon_{\lambda}^{\nu} (P)$, where Λ_{μ}^{ν} is the Lorentz transformation which takes a meson at rest to momentum P . At the same time, we use the transformation law for Dirac matrices,

$$\frac{(M + \not{P} \gamma_0) \gamma_{\mu} (M + \gamma_0 \not{P})}{2M (E + M)} = \Lambda_{\mu}^{\nu} \gamma_{\nu} \quad , \text{ so that we may finally write}$$

$$\text{the wave function in the simple form } \frac{- \not{\epsilon}_{\lambda} (P)}{2 \sqrt{2}} \left(\frac{\not{P}}{M} - 1\right) .$$

We now have the spin part of the meson wave functions and we need only to specify the SU(3) quantum numbers of the quarks. To do this we use the 3 x 3 SU(3) matrices M_{α}^{β} . The rows and columns of these matrices, respectively, tell which quark and antiquark compose the meson. We therefore have

$$\frac{- ((\not{P} + M) \gamma_5)_{m_1 m_2}}{2 \sqrt{2} M} M_{\alpha}^{\beta} \quad \text{for pseudoscalar mesons}$$

$$\frac{((\not{P} + M) \not{\epsilon})_{m_1 m_2}}{2 \sqrt{2} M} M_{\alpha}^{\beta} \quad \text{for vector mesons.}$$

The adjoint wave function, which corresponds to $u \rightarrow \bar{u}$, $\bar{v} \rightarrow v$, is gotten by substituting $P \rightarrow -P$, $M \rightarrow M^+$, and $\epsilon_{\lambda} \rightarrow \epsilon_{\lambda}^*$.

We will now consider the baryon wave functions, which are of the form $u_{\sigma_1} (P)_{m_1} u_{\sigma_2} (P)_{m_2} u_{\sigma_3} (P)_{m_3}$. Here m_i indexes the four

components of the Dirac spinor. Again we will find that summing over the values of $\sigma_1, \sigma_2, \sigma_3$ corresponding to a state of definite spin results in an expression which can be written quite simply. For example,
$$\frac{(u_+ u_- - u_- u_+) u_{\sigma_3}}{\sqrt{2}}$$
 is the wave function for a baryon with

spin $1/2$ and $s_2 = \sigma_3$. This is so because the first two quarks are in a spin zero state so the total spin is that of the third quark. The expression for two quarks in a spin zero state can be simplified in the same manner used for a quark and an antiquark in a spin zero state. But it is simpler to use the relation $u_{\sigma} (P)_{m_i} = \bar{v}_{\sigma} (P)_{m_j} C_{m_j m_i}$, where $C = -i \gamma^y \gamma^o$. We can then use the results for combining u and \bar{v} spinors, which we got above, to write

$$\frac{u_+ u_- - u_- u_+}{\sqrt{2}} = \frac{(u_+ \bar{v}_- - u_- \bar{v}_+) C}{\sqrt{2}} = \frac{-((\not{P} + M) \gamma_5 C)}{2 \sqrt{2} M} .$$

$$\text{Therefore } \left(\frac{u_+ u_- - u_- u_+}{\sqrt{2}} \right) u_{\sigma_3} = \frac{-1}{2 \sqrt{2} M} \left((\not{P} + M) \gamma_5 C \right)_{m_1 m_2} u_{\sigma_3} (P)_{m_3} .$$

This is the wave function for 3 quarks in a spin $1/2$ state, where we have chosen to put the first two in a spin zero state. As in the case of meson wave functions, the value of the wave function for a particular choice of $\alpha_1, \alpha_2,$ and α_3 is simply the amplitude for the three quarks to have the indices of their Dirac spinors equal to $\alpha_1, \alpha_2,$ and α_3 respectively. One can remember this wave function by

noting that the wave function of quarks one and two,

$$\frac{-1}{2\sqrt{2}M} ((\not{P} + M) \gamma_5 C)_{m_1 m_2},$$

is an invariant and carries no information about the spin of the baryon. The wave function of the third quark carries the information about the spin of the baryon;

this is clear because $u_{\sigma_3}(P)$ is the Dirac spinor which one commonly uses to represent a spin 1/2 baryon with $s_2 = \sigma_3$.

The procedure we just used was to single out two quarks, put them in a definite spin state, use our meson results for the wave function of the two quarks, and then include the wave function of the third quark. In a similar manner, we will now construct the wave function for a baryon with quark spin 3/2. First, we put 2 quarks in a symmetric or spin one state. Using $u_{\sigma}(P)_{m_i} = \bar{v}_{\sigma}(P)_{m_j} C_{m_j m_i}$, and our results for vector mesons, we can write the wave function for this state as

$$-\frac{(\not{\epsilon}_{\lambda} (\not{P} - M) C)_{m_1 m_2}}{M}.$$

Here λ is the spin of the 2 quarks along the Z axis. We may combine this with the wave function of the third quark to give

$$-\frac{(\not{\epsilon}_{\lambda} (\not{P} - M) C)_{m_1 m_2} u_{\sigma_3}(P)_{m_3}}{M},$$

which is the product of a spin one wave function and a spin 1/2 wave function. The spin 3/2 part of this combination may be obtained with the aid of the Clebsch-Gordan coefficient $\left[1 \ 1/2 \ 3/2 \right]_{\sigma}^{\lambda \sigma_3}$

for combining spin one, $s_2 = \lambda$, with spin 1/2, $s_2 = \sigma_3$, to give spin 3/2, $s_2 = \sigma$. We then have

$$- \frac{1}{2 \sqrt{2} M} \left(\not{\epsilon}_\lambda (\not{P} - M) C \right)_{m_1 m_2} u_\sigma (P)_{m_3} \left[1 \ 1/2 \ 3/2 \right]_{\sigma}^{\lambda \sigma_3}$$

as the wave function for a quark-spin 3/2 particle with $s_2 = \sigma = \lambda + \sigma_3$.

A simpler form is

$$\frac{1}{2 \sqrt{2} M} (\gamma_\nu (M - \not{P}) C)_{m_1 m_2} u_{m_3}^\nu,$$

where

$$u_{m_3}^\nu = u_{\sigma_3} (P)_{m_3} \epsilon_\lambda^\mu \left[1 \ 1/2 \ 3/2 \right]_{\sigma}^{\lambda \sigma_3}$$

is a Rarita-Schwinger vector-spinor, and we shall use this form in what follows. We now have the quark spin 1/2 and quark spin 3/2 baryon wave functions, and we can combine them with the SU(3) quantum numbers of the quarks to give SU(6) wave functions. These are

$$- \frac{1}{2\sqrt{2}} \frac{((\not{P} + M) \gamma_S C)_{m_1 m_2} u_\sigma (P)_{m_3} (q_1)_{\alpha_1} (q_2)_{\alpha_2} (q_3)_{\alpha_3}}{M}$$

quark spin 1/2, and

$$- \frac{1}{2\sqrt{2} M} (\gamma_\nu (\not{P} - M) C)_{m_1 m_2} u_\sigma (P)_{m_3} (q_1)_{\alpha_1} (q_2)_{\alpha_2} (q_3)_{\alpha_3}$$

quark spin 3/2.

(q_i) is a 3 dimensional column vector whose first, second, and third elements are the amplitudes for the i^{th} quark to be a proton, neutron or lambda-like quark, respectively. Each quark can be in any of six states, so there are $6 \times 6 \times 6 = 216$ states possible for three quarks.

It is useful to group these according to the overall symmetry of the wave function under interchange of two quarks. That is, there are 56 totally symmetric states, 20 totally antisymmetric states, and 2 groups with mixed symmetry, and 70 states each. This grouping is convenient because an $SU(6)$ rotation, i.e., a rotation of the six dimensional space in which the quarks live, rotates the states of each group among themselves, leaving the overall symmetry of the wave function unchanged. We will now list the wave functions of the various $SU(6)$ multiplets. In the following, B denotes the 3×3 baryon matrix whose elements were given in Part 2, while $D_{\alpha_1 \alpha_2 \alpha_3}$ is the $SU(3)$ decimet wave function also given in Part 2.

We begin with the wave functions of the 56, which contain an octet of quark spin 1/2, and a decimet of quark spin 3/2.

56, octet, quark spin 1/2:

$$-\frac{1}{6\sqrt{2}M} \left\{ \begin{array}{l} (\gamma_5 (M - \not{P}) C)_{m_1 m_2} u_\sigma (P)_{m_3} \epsilon_{\alpha_1 \alpha_2 q} B_{\alpha_3}^q \\ + (\gamma_5 (M - \not{P}) C)_{m_1 m_3} u_\sigma (P)_{m_2} \epsilon_{\alpha_1 \alpha_3 q} B_{\alpha_2}^q \\ + (\gamma_5 (M - \not{P}) C)_{m_2 m_3} u_\sigma (P)_{m_1} \epsilon_{\alpha_2 \alpha_3 q} B_{\alpha_1}^q \end{array} \right\}$$

56, decimet, quark spin 3/2:

$$\frac{1}{2\sqrt{2}M} (\gamma_5 (M - \not{P}) C)_{m_1 m_2} u_{m_3}^{\nu} D_{\alpha_1 \alpha_2 \alpha_3}$$

There are two 70's. In order to see their symmetry, let us pretend that there is a vector v_i associated with the i^{th} quark. Then the vector $\eta \equiv \frac{r_2 - r_1}{\sqrt{2}}$ is antisymmetric under interchange of quarks one and two, while the vector $\xi \equiv \frac{r_1 + r_2 - 2r_3}{\sqrt{6}}$ is symmetric under interchange of one and two. Under interchange of one and three, or two and three, they mix. We may construct our 70's so that under interchange of any two quarks, they transform just like η and ξ . Essentially this means we construct states which are either symmetric (η) or antisymmetric (ξ) in quarks one and two, but orthogonal to states with total symmetry or total antisymmetry. Each 70 consists of an octet of quark spin 3/2, an octet of quark spin 1/2, a decimet of quark spin 1/2, and a singlet of quark spin 1/2. We list the 70 wave functions below.

70, decimet, quark spin 1/2:

" η " type

$$\frac{1}{3\sqrt{2}M} \left\{ \begin{array}{l} (\gamma_5 (M - \not{P}) C)_{m_1 m_2} u_{m_3} \\ + 1/2 (\gamma_5 (M - \not{P}) C)_{m_1 m_3} u_{m_2} \\ - 1/2 (\gamma_5 (M - \not{P}) C)_{m_2 m_3} u_{m_1} \end{array} \right\} D_{\alpha_1 \alpha_2 \alpha_3}$$

"ξ" type

$$\frac{1}{2\sqrt{6}M} \left\{ \begin{array}{l} (\gamma_5 (M - \not{P}) C)_{m_1 m_3} u_{m_2} \\ (\gamma_5 (M - \not{P}) C)_{m_2 m_3} u_{m_1} \end{array} \right\} D_{\alpha_1 \alpha_2 \alpha_3}$$

70, octet, quark spin 3/2

"η" type

$$\frac{1}{6M} (\gamma_\mu (M - \not{P}) C)_{m_1 m_3} u_{m_2}^\mu (\epsilon_{\alpha_1 \alpha_2 q} B_{\alpha_3}^q + \\ + 1/2 \epsilon_{\alpha_1 \alpha_3 q} B_{\alpha_2}^q - 1/2 \epsilon_{\alpha_2 \alpha_3 q} B_{\alpha_1}^q)$$

"ξ" type

$$\frac{1}{4\sqrt{3}M} (\gamma_\mu (M - \not{P}) C)_{m_1 m_3} u_{m_2}^\mu (\epsilon_{\alpha_1 \alpha_3 q} B_{\alpha_2}^q + \epsilon_{\alpha_2 \alpha_3 q} B_{\alpha_1}^q)$$

70, octet or singlet, quark spin 1/2

"η" type

$$\frac{-1}{2\sqrt{6}M} \left\{ \begin{array}{l} (\gamma_5 (M - \not{P}) C)_{m_1 m_3} u_{m_2} B_{\alpha_2}^q \epsilon_{\alpha_1 \alpha_3 q} \\ - (\gamma_5 (M - \not{P}) C)_{m_2 m_3} u_{m_1} B_{\alpha_1}^q \epsilon_{\alpha_2 \alpha_3 q} \end{array} \right\}$$

"ξ" type

$$\frac{1}{6\sqrt{2}M} \left(\begin{array}{l} 2 (\gamma_5 (M - \not{P}) C)_{m_1 m_2} u_{m_3} B_{\alpha_3}^q \epsilon_{\alpha_1 \alpha_2 q} \\ - (\gamma_5 (M - \not{P}) C)_{m_1 m_3} u_{m_2} B_{\alpha_2}^q \epsilon_{\alpha_1 \alpha_3 q} \\ - (\gamma_5 (M - \not{P}) C)_{m_2 m_3} u_{m_1} B_{\alpha_1}^q \epsilon_{\alpha_2 \alpha_3 q} \end{array} \right)$$

We also have 20 antisymmetric states, consisting of a singlet of quark spin 3/2, and an octet of quark spin 1/2. We list their wave functions.

20, singlet, quark spin 3/2

$$\frac{1}{4\sqrt{3}M} (\gamma_\mu (M - \not{P}) C)_{m_1 m_2} u_{m_3}, \quad \mu \epsilon_{\alpha_1 \alpha_2 \alpha_3}$$

20, octet, quark spin 1/2

$$\frac{1}{6\sqrt{6}M} \left(\begin{array}{l} (\gamma_5 (M - \not{P}) C)_{m_1 m_3} u_{m_2} (\epsilon_{\alpha_1 \alpha_2 q} B_{\alpha_3}^q - \epsilon_{\alpha_2 \alpha_3} B_{\alpha_1}^q) \\ (\gamma_5 (M - \not{P}) C)_{m_2 m_3} u_{m_1} (\epsilon_{\alpha_1 \alpha_2 q} B_{\alpha_3}^q - \epsilon_{\alpha_3 \alpha_1} B_{\alpha_2}^q) \\ + (\gamma_5 (M - \not{P}) C)_{m_1 m_2} u_{m_3} (\epsilon_{\alpha_3 \alpha_1 q} B_{\alpha_2}^q - \epsilon_{\alpha_2 \alpha_3 q} B_{\alpha_1}^q) \end{array} \right)$$

This completes our list of SU(6) wave functions for three quarks composing a baryon. To calculate vertex amplitudes we refer to Figure 3. With each line connecting an incoming quark and an

outgoing quark, we associate the scalar product of the SU(6) wave functions of the two quarks. Similarly, with the line corresponding to quark-antiquark annihilation, we associate the scalar product of the SU(6) wave functions of the quark and antiquark. This leads to the expression $\bar{\psi}^{abd} M_d^c \psi_{abc}$ for meson-baryon vertices. ψ_{abc} is the SU(6) wave function for the three quarks in the incoming baryon, M_d^c is the SU(6) wave function for the quark and antiquark in the meson, and $\bar{\psi}^{abd}$ is the adjoint wave function of the baryon which is going out. For mesons, we must add the amplitudes associated with the graphs in Figures 6 and 7. We get $M_{1c}^{+b} M_{2b}^a M_{3a}^c$ for the graph in Figure 6, and $M_{1a}^{+d} M_{3d}^c M_{2c}^a$ for the graph in Figure 7. These rules lead to the vertex in Table 3.

Up to now we have only considered quark graphs for vertices. However, we can also write down quark graphs for scattering amplitudes, and it is natural to ask what we can say about them. For example, in Figure 8 we give a Feynman diagram for meson-meson scattering via meson exchange. In Figure 9 we give a quark graph which might also represent such a process. We would like to find simple rules for using the graph in Figure 9 to get the amplitude for the process. The amplitude for the process is

$$\frac{\langle M_3 M_4 M_i \rangle \langle M_i^+ M_1 M_2 \rangle}{t - M_i^2} + \text{symmetrization in } 1 \text{ \& } 2 \text{ and } 3 \text{ \& } 4.$$

The M 's are our $SU(6)$ wave functions. In the limit of $SU(6)$ symmetry, M_i is the same for all 36 $q\bar{q}$ states. We therefore may sum over all orientations of the quarks in spin and $SU(3)$ space. We have, since M_i is of the form $u_\sigma \bar{v}_\sigma$,

$$\begin{aligned} & \langle M_3 M_4 u_\sigma \bar{v}_\sigma \rangle \langle v_\sigma \bar{u}_\sigma M_1 M_2 \rangle \frac{1}{t - M_i^2} = \\ & = (M_3 M_4)_\alpha^\beta \left(\frac{\not{P} + M}{2M} \right)_\beta^\gamma (M_1 M_2)_\gamma^\delta \left(\frac{\not{P} - M}{2M} \right)_\delta^\alpha \left(\frac{1}{t - M_i^2} \right) = \\ & = \left(M_3 M_4 \left(\frac{\not{P} + M}{2M} \right) M_1 M_2 \left(\frac{\not{P} - M}{2M} \right) \right) \frac{1}{t - M^2} \end{aligned}$$

Thus we see that the first term in the $SU(6)_W$ amplitude for meson exchange corresponds to putting $\frac{\not{P} + M}{2M}$ and $\frac{\not{P} - M}{2M}$ on the exchanged quark and antiquark lines, respectively, and meson wave functions on external $q\bar{q}$ lines associated with a meson. We then take the scalar product. We see that $SU(6)_W$ leads in to a simple form for quark graphs associated with meson exchange.

Next, we will examine the Regge behavior of this amplitude. At very high s , $\frac{\not{P}}{2M}$ is a flip term, while 1 is nonflip, that is, \not{P} flips one unit of quark spin. Therefore, terms with odd powers of M are flip-nonflip, or nonflip-flip, while terms with even powers of M are nonflip-nonflip or flip-flip. Reggeization will result in there being cuts in either nonflip-nonflip and flip-flip, or in

nonflip-flip and flip-nonflip. This is just the behavior we found in Part II. Thus we see from the quark graph picture how the cuts arise and in which amplitudes.

TABLE 1

Baryon-Baryon-Meson Vertices

Vertex	Spins [†]	Value [*]
BBP	1/2, 1/2, 0	$\frac{1}{18} [5 \langle \bar{B}PB \rangle + \langle \bar{B}BP \rangle]$
BBV	1/2, -1/2, 1	$\frac{1}{9\sqrt{2}} [5 \langle \bar{B}VB \rangle + \langle \bar{B}BV \rangle - \langle \bar{B}B \rangle \langle V \rangle]$
	1/2, 1/2, 0	$\frac{1}{6} [\langle \bar{B}VB \rangle - \langle \bar{B}BV \rangle + \langle \bar{B}B \rangle \langle V \rangle]$
DBP	1/2, 1/2, 0	$-\frac{1}{3}\sqrt{\frac{2}{3}} \left[\bar{D}_{\alpha\beta\gamma} \epsilon^{\beta\delta\tau} B_{\tau}^{\alpha} P_{\delta}^{\gamma} \right]$
DBV	3/2, 1/2, 1	$\frac{1}{3} \left[\bar{D}_{\alpha\beta\gamma} \epsilon^{\beta\delta\tau} B_{\tau}^{\alpha} V_{\delta}^{\gamma} \right]$
	1/2, 1/2, 0	0
	1/2, -1/2, 1	$\frac{1}{3\sqrt{3}} \left[\bar{D}_{\alpha\beta\gamma} \epsilon^{\beta\delta\tau} B_{\tau}^{\alpha} V_{\delta}^{\gamma} \right]$
DDP	3/2, 3/2, 0	$\frac{1}{2} \left[\bar{D}_{\alpha\beta\gamma} D^{\alpha\beta\delta} P_{\delta}^{\gamma} \right]$
	1/2, 1/2, 0	$\frac{1}{6} \left[\bar{D}_{\alpha\beta\gamma} D^{\alpha\beta\delta} P_{\delta}^{\gamma} \right]$
DDV	3/2, 3/2, 0	$\frac{1}{2} \left[\bar{D}_{\alpha\beta\gamma} D^{\alpha\beta\delta} V_{\delta}^{\gamma} \right]$
	3/2, 1/2, 1	$\frac{1}{\sqrt{6}} \left[\bar{D}_{\alpha\beta\gamma} D^{\alpha\beta\delta} V_{\delta}^{\gamma} \right]$
	1/2, 1/2, 0	$\frac{1}{2} \left[\bar{D}_{\alpha\beta\gamma} D^{\alpha\beta\delta} V_{\delta}^{\gamma} \right]$
	1/2, -1/2, 1	$\frac{\sqrt{2}}{3} \left[\bar{D}_{\alpha\beta\gamma} D^{\alpha\beta\delta} V_{\delta}^{\gamma} \right]$
	1/2, 3/2, -1	$\frac{1}{\sqrt{6}} \left[\bar{D}_{\alpha\beta\gamma} D^{\alpha\beta\delta} V_{\delta}^{\gamma} \right]$

[†] Particle 1 is outgoing; particles 2 and 3, incoming.

^{*} $\bar{B}PB$ denotes $\bar{B}_{\beta}^{\alpha} P_{\gamma}^{\beta} B_{\alpha}^{\gamma}$.

TABLE 2

Meson-Meson-Meson Vertices

Vertex	Spins	Value
$P_1 P_2 V$	0, 0, 0	$\frac{1}{2} [\langle P_1 P_2 V \rangle - \langle P_1 V P_2 \rangle]$
$V_1 V_2 P$	1, 1, 0	$\frac{1}{2} [\langle V_1 V_2 P \rangle + \langle V_1 P V_2 \rangle]$
$V_1 V_2 V_3$	0, 0, 0	$\frac{1}{2} [\langle V_1 V_2 V_3 \rangle - \langle V_3 V_2 V_1 \rangle]$
	1, 1, 0	$\frac{1}{2} [\langle V_1 V_2 V_3 \rangle - \langle V_3 V_2 V_1 \rangle]$
	1, 0, 1	$\frac{1}{2} [\langle V_1 V_2 V_3 \rangle - \langle V_3 V_2 V_1 \rangle]$
	0, 1, -1	$\frac{1}{2} [\langle V_1 V_2 V_3 \rangle - \langle V_3 V_2 V_1 \rangle]$

TABLE 3

Invariant Vertex Functions

Vertex	Function*
BBP	$\frac{c}{9} \left[(M_1+M_2)^2 - M_3^2 \right] (\bar{u}_1 \gamma_5 u_2) \left[5 \langle \bar{B}PB \rangle + \langle \bar{B}BP \rangle \right]$
BBV	$\frac{c}{9} \left\{ \epsilon_3 \cdot (p_1+p_2) (\bar{u}_1 u_2) \left[(M_1+M_2) (5 \langle \bar{B}VB \rangle + \langle \bar{B}BV \rangle - \langle \bar{B}B \rangle \langle V \rangle) - 3M_3 (\langle \bar{B}VB \rangle - \langle \bar{B}BV \rangle + \langle \bar{B}B \rangle \langle V \rangle) \right] \right.$ $\left. - (\bar{u}_1 \not{\epsilon}_3 u_2) \left[(M_1+M_2)^2 - M_3^2 \right] \left[5 \langle \bar{B}VB \rangle + \langle \bar{B}BV \rangle - \langle \bar{B}B \rangle \langle V \rangle \right] \right\}$
DBP	$+\frac{4c}{3} M_1 P_{2\mu} (\bar{u}_{1\mu} u_2) \left[D_{\alpha\beta\gamma} \epsilon^{\beta\delta\tau} B_{\tau}^{\alpha} P_{\delta}^{\gamma} \right]$
DBV	$-\frac{2c}{3} \left\{ \left[(M_1+M_2)^2 - M_3^2 \right] \epsilon_{3\mu} (\bar{u}_{1\mu} \gamma_5 u_2) - P_{1\mu} (\bar{u}_{1\mu} \gamma_5 u_2) \epsilon_3 \cdot (p_1+p_2) \right.$ $\left. + 2 M_1 P_{2\mu} (\bar{u}_{1\mu} \not{\epsilon}_3 \gamma_5 u_2) \right\} \left[\bar{D}_{\alpha\beta\gamma} \epsilon^{\beta\delta\tau} B_{\tau}^{\alpha} V_{\delta}^{\gamma} \right]$
DDP	$c \left\{ 2 P_{2\mu} (\bar{u}_{1\mu} \gamma_5 u_{2\nu}) P_{1\nu} - \left[(M_1+M_2)^2 - M_3^2 \right] (\bar{u}_{1\mu} \gamma_5 u_{2\mu}) \right\} \bar{D}_{\alpha\beta\gamma} D^{\alpha\beta\delta} P_{\delta}^{\gamma}$
DDV	$c \left\{ (M_1+M_2)^2 - M_3^2 (\bar{u}_{1\mu} \not{\epsilon}_3 u_{2\mu}) - M_1+M_2-M_3 (\bar{u}_{1\mu} u_{2\mu}) \epsilon_3 \cdot (p_1+p_2) - 2 P_{2\mu} (\bar{u}_{1\mu} \not{\epsilon}_3 u_{2\nu}) P_{1\nu} \right.$ $\left. + \frac{2 P_{2\mu} (\bar{u}_{1\mu} u_{2\nu}) P_{1\nu} \epsilon_3 \cdot (p_1+p_2)}{M_1+M_2+M_3} \right\} \left[\bar{D}_{\alpha\beta\gamma} D^{\alpha\beta\delta} V_{\delta}^{\gamma} \right]$
$P_1 P_2 V$	$- d M_3 \epsilon_3 \cdot (p_1+p_2) \langle P_1 P_2 V \rangle - \langle P_1 V P_2 \rangle$

TABLE 3 (cont.)

Vertex	Function*
$V_{12}VP$	$-i d \epsilon^{\mu\nu\rho\sigma} p_{3\mu} (p_1+p_2)_\nu \epsilon_{2\rho} \epsilon_{1\sigma} \left[\langle V_{12}VP \rangle + \langle V_{1PV_2} \rangle \right]$
$V_{12}VV_3$	$d \left[M_3 (\epsilon_1^* \cdot \epsilon_2) (\epsilon_3 \cdot (p_1+p_2)) - M_2 (\epsilon_1^* \cdot \epsilon_3) (\epsilon_2 \cdot (p_3+p_1)) - M_1 (\epsilon_2 \cdot \epsilon_3) (\epsilon_1^* \cdot (p_2-p_3)) \right.$ $\left. + \frac{\epsilon_1^* \cdot (p_2-p_3) \epsilon_2 \cdot (p_3+p_1) \epsilon_3 \cdot (p_1+p_2)}{2(M_1 + M_2 + M_3)} \right] \left[\langle V_{12}VV_3 \rangle - \langle V_{3V_2V_1} \rangle \right]$

* M_i and p_i refer to the mass and momentum of the i -th particle, $i = 1, 2, 3$. Particle 1 is outgoing; particles 2 and 3 incoming.

TABLE 4Odd powers of $m(J)$ in vector meson vertices.

<u>Vertex</u>	<u>V* Helicity</u>	<u>m(J) Factors</u>
$NN\rho^*$	± 1	$c(J)$
	0	$m(J) c(J)$
$\Delta N\rho^*$	± 1 (a)	$c(J)$
$NN\omega^*$	± 1	$c(J)$
	0	$m(J) c(J)$
$\pi\pi\rho^*$	0 (b)	$m(J) d(J)$
$\pi\rho\omega^*$	± 1 (b)	$d(J)$
$\pi\omega\rho^*$	± 1 (b)	$d(J)$
$\eta\rho\rho^*$	± 1 (b)	$d(J)$

(a) Only helicities allowed by $SU(6)_W$.

(b) Only helicities allowed by parity and angular momentum.

TABLE 5

Wrong signature nonsense dips for vector meson exchange.

31

Reaction	Exchange	Helicities	Relative Magnitude	Cut?	Dip?
$\pi^- p \rightarrow \pi^0 n$	ρ	1, 0	$5\sqrt{2} \sqrt{t} g(J)$	none	yes
$\pi^- p \rightarrow \omega n$	ρ	0, 0	$3\sqrt{2} m(J) g(J)$	weak	
$\pi^+ p \rightarrow \pi^0 \Delta^{++}$	ρ	1, 1	$5 t g(J)/m(J)$	strong	no
$\pi^+ p \rightarrow \omega \Delta^{++}$	ρ	0, 1	$3\sqrt{t} g(J)$	none	
$\pi^0 p \rightarrow \rho^0 p$	ρ	$1(3/2, 1/2), 0$	$6\sqrt{t} g(J)$	none	yes
$\rho^0 p \rightarrow \pi^0 p$	ρ	$1(1/2, -1/2), 0$	$2\sqrt{3} \sqrt{t} g(J)$	none	
$\rho^0 p \rightarrow \eta p$	ρ	$1(3/2, 1/2), 1$	$3\sqrt{2} t g(J)/m(J)$	strong	no
$\omega p \rightarrow \pi^+ n$	ρ	$1(1/2, -1/2), 1$	$\sqrt{6} t g(J)/m(J)$	strong	
	ω	1, 1	$(3/\sqrt{2}) t g(J)/m(J)$	strong	yes ^a
	ω	0, 1	$(9/\sqrt{2}) \sqrt{t} g(J)$	none	
	ρ	1, 1	$(3/\sqrt{2}) t g(J)/m(J)$	strong	yes ^b
	ρ	0, 1	$(9/\sqrt{2}) \sqrt{t} g(J)$	none	
	ρ	1, 1	$(5/\sqrt{6}) t g(J)/m(J)$	strong	no ^c
	ρ	0, 1	$(3/\sqrt{6}) \sqrt{t} g(J)$	none	
	ρ	1, 1	$5 t g(J)/m(J)$	strong	no ^d
	ρ	0, 1	$3\sqrt{t} g(J)$	none	

TABLE 5 (cont.)

$$a) \quad \frac{d\sigma}{dt} (\pi^+ p \rightarrow \rho^+ p) + \frac{d\sigma}{dt} (\pi^- p \rightarrow \rho^- p) - \frac{d\sigma}{dt} (\pi^- p \rightarrow \rho^0 n)$$

$$b) \quad \frac{d\sigma}{dt} (\gamma p \rightarrow \pi^0 p)$$

$$c) \quad \frac{d\sigma}{dt} (\gamma p \rightarrow \eta p)$$

$$d) \quad \frac{d\sigma}{dt} (\gamma p \rightarrow \pi^+ n) - \frac{d\sigma}{dt} (\gamma n \rightarrow \pi^- p)$$

REFERENCES

1. V.N. Gribov, Zh. Eksperim. i Teor. Fiz. 43, 152 (1962) [translation: Soviet Phys.-JETP 16, 1080 (1963)].
2. S.W. MacDowell, Phys. Rev. 116, 774 (1959).
3. V. Barger and D. Cline, Phys. Letters 26B, 85 (1967), suggest that only the lowest state on each MacDowell twin is suppressed. This ad hoc assumption has also been made in Veneziano models of πN scattering, which have failed to fit backward scattering data even qualitatively. See, e.g., S. Chu and B.R. Desai, University of California at Riverside Report No. UCR-34P107-96 (to be published).
4. The fixed cut gives the trajectory functions a two-sheeted J-plane structure. In an analytic continuation from $E > 0$ to $E < 0$, the Regge poles move from one sheet of the J-plane to the other. See V. Singh, Phys. Rev. 127, 632 (1962).
5. L. Van Hove, Phys. Letters 24B, 183 (1967); R.P. Feynman, unpublished.
6. The total momentum in the u channel is denoted by k_μ , and p_μ and p'_μ are the initial and final nucleon momenta, respectively. The energy, momentum, and scattering angle in the u channel center of mass are $W(=\sqrt{u})$, p , and z_u .
7. The factor $\left[\frac{k}{m(\lambda)} - m(\lambda) \right] / m(\lambda)$ corresponds to a normalization $\bar{u}_\lambda u_\lambda = 2$, independent of λ .

8. Properly speaking, we should work with Legendre functions of the second kind to make an analytic continuation to the left of $\text{Re } \ell = -\frac{1}{2}$.
9. In general, we expect $g^2(\ell)$ to be a meromorphic function of $m(\ell)$. Even powers of $m(\ell)$ yield a fixed cut in the spin-flip amplitude, while odd powers give a fixed cut in the nonflip amplitude. Nucleon exchange in backward π^+p scattering may be qualitatively fitted with only even powers of $m(\ell)$ in $g^2(\ell)$.
10. The contribution of the Feynman diagram for the exchange of an unnatural parity resonance has the form of (1) with $m(\ell)$ replaced by $-m(\ell)$. $\mathcal{N}(m(\ell)) + \mathcal{N}(-m(\ell))$ has no odd powers of $m(\ell)$ and hence no cut in ℓ .
11. R.L. Sugar and J.D. Sullivan, Phys. Rev. 166, 1515 (1968)
12. See D.L. Steele, thesis, University of Illinois, 1969 (unpublished).
13. If $g^2(\alpha_0) = 0$, there would be no infinity in (7) and no auxiliary pole $\alpha_2(u)$. However, the Regge pole contribution to the nonflip part of \mathcal{N} at $u = 0$ would be of order $b(u)$, which by assumption is small. Nucleon-exchange data in backward π^+p scattering show no indication of any dip at $u = 0$. (See also Ref. 9.)
14. Note that α_1 and α_2 collide at $u = 0$ and become complex for $u < 0$. If there is only one moving pole (see Ref. 13), then α does not become complex. Also note that $\alpha_{1,2}(0)$ no longer coincide with the branch point α_0 .

15. See, for example, rapporteur talks of B. French and A. Donnachie in Proceedings of 14th International Conference on High Energy Physics (CERN, Geneva, 1968).
16. $SU(6)_W$ was first proposed by H.J. Lipkin and S. Meshkov, Phys. Rev. Letters 14, 670 (1965).
17. A good review of $SU(6)_W$ is given in H. Harari's lectures in Lectures in Theoretical Physics (University of Colorado Press, Boulder, Colorado, 1965), Vol. VIII-B.
18. $SU(6)_W$ is, of course, meaningless for non-collinear processes. If we admit the idea of Regge pole dominance and factorization, we can see why it does not work for collinear processes either. This is because $SU(6)_W$ relates spin nonflip amplitudes, and the latter vanish as a consequence of factorization.
19. See R. Delbourgo and H. Rashid, Phys. Rev. 176, 2074 (1968). They give a model with $SU(6)_W$ symmetric vertices and no Regge cuts, but find it necessary to use parity-doubled quarks to eliminate \sqrt{t} singularities. In our model, these singularities are cancelled by the cut terms.
20. G. Zweig, CERN Report Th-402 (1964), unpublished.
21. H. Harari, Phys. Rev. Letters 22, 562 (1969).
22. J. Rosner, Phys. Rev. Letters 22, 689 (1969).
23. Normal $SU(6)$ is clearly not an appropriate symmetry for the vertices, for it requires a $q\bar{q}$ pair to annihilate in a singlet spin state--contrary to angular momentum and parity conservation.

24. See B.W. Lee's lectures in Particle Symmetries, (Gordon and Breach, New York, 1966).
25. We have calculated the entries in Table 3 by selecting a complete set of invariant vertex functions, evaluating these functions in a collinear frame, equating these values to those in Tables 1 and 2, and solving the resulting set of linear equations. An alternate method would be to construct relativistic wave functions and write down a covariant version of (1). See B. Sakita and K.C. Wali, Phys. Rev. 139, B1355 (1965).
26. For a meson with four-momentum $(E; 0, 0, q)$, $E^2 - q^2 = M_V^2$, the normalized polarization vector is $\epsilon^0 = (q; 0, 0, E)/M_V$.
27. Details of the Van Hove construction are discussed by R. Blankenbecler and R.L. Sugar, Phys. Rev. 168, 1597 (1968).
28. There is an ambiguity in the Van Hove model of Reggeization corresponding to the ambiguity in the behavior of the propagator and vertex functions off the mass shell. We eliminate this ambiguity by choosing to Reggeize t-channel helicity amplitudes and including in the Van Hove sum (16) terms whose only t dependence is in the denominator $t - m(J)^2$.
29. This may not occur until quite high energies. From Eq. (26) we see that the leading term in the asymptotic expansion of the cut dominates only when $\alpha' t \ln s \gg 1$.
30. Note that our approach to wrong-signature nonsense dips is compatible with the argument that the exchange of a pair of exchange

degenerate trajectories will produce no dip.

31. Photoproduction processes are included in Table 5 assuming vector dominance. This is an unambiguous procedure for the reactions listed because the VVP vertex is automatically gauge invariant.
32. A summary of the data and an empirical rule for the presence of wrong-signature nonsense dips in vector exchange processes are given in a review talk on photoproduction by H. Harari at the Fourth International Symposium on Electron and Photon Interactions at High Energies (Liverpool, England; September 1969), unpublished.

FIGURE CAPTIONS

- Figure 1 : Dashed line - initial contour; solid line - opened contour.
- Figure 2 : Pole trajectory for f^+ . Dashed lines show path on second sheet; solid lines refer to the principal sheet.
- Figure 3 : Quark graph for meson-baryon vertex
- Figure 4 : Kinematics for $\pi\pi \rightarrow \pi\omega$.
- Figure 5 : Dashed line - initial contour; solid line - opened contour.
- Figures 6
and 7: Quark graphs for meson vertices.
- Figure 8 : Feynman diagram for meson scattering via exchange of intermediate meson.
- Figure 9 : Quark graph corresponding to Feynman diagram of Figure 8.

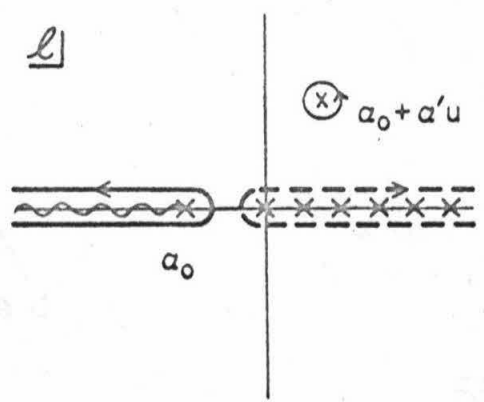


Fig. 1

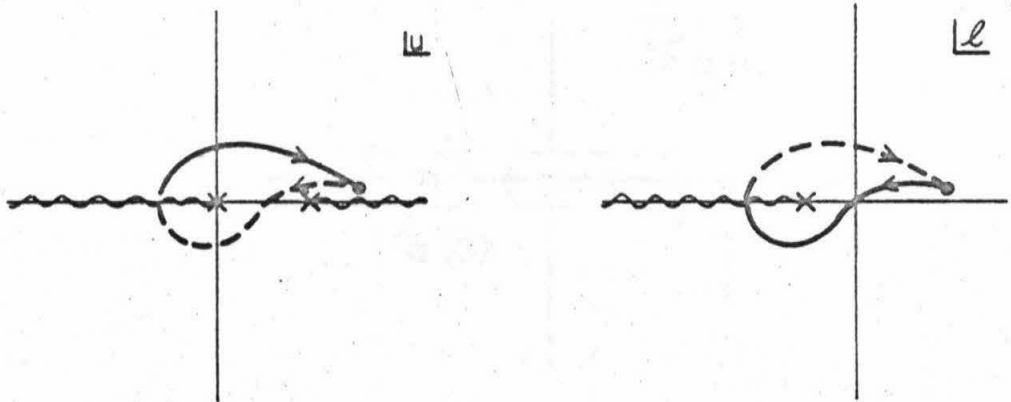


Fig. 2

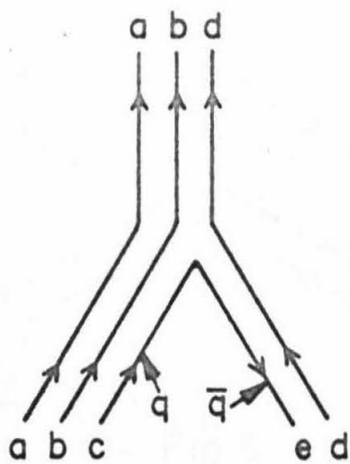


Fig. 3

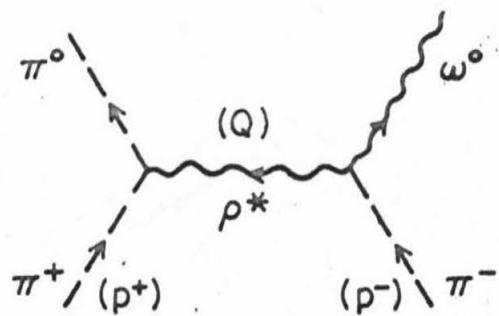


Fig. 4

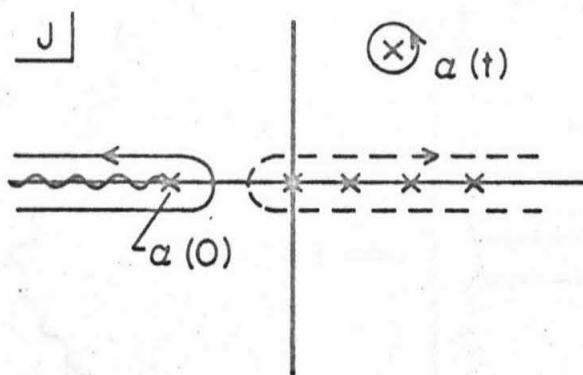


Fig. 5

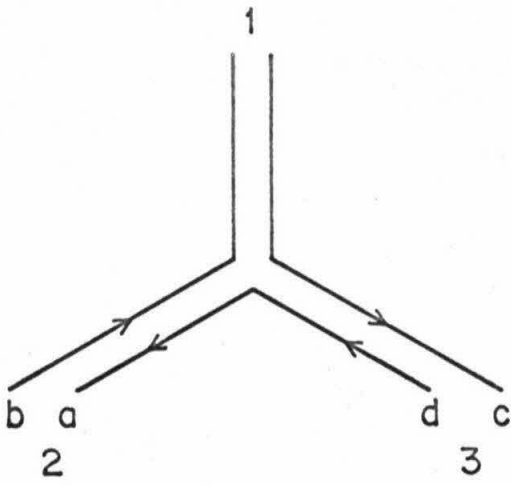


Fig. 6

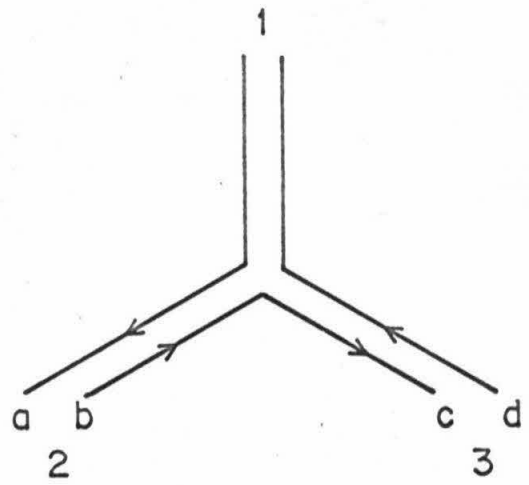


Fig. 7

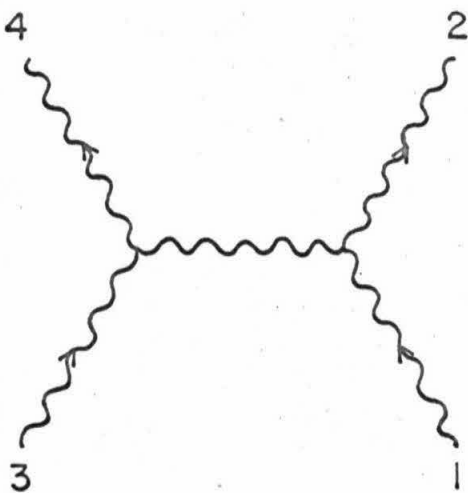


Fig. 8

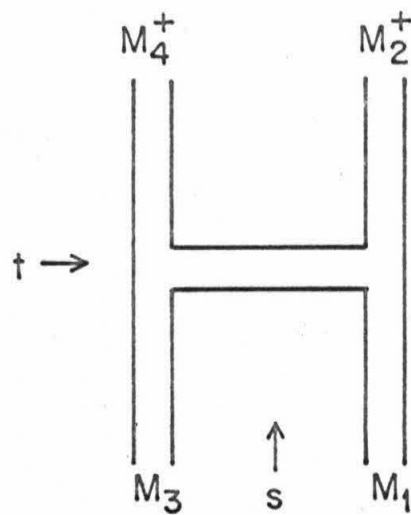


Fig. 9